applied sciences

MDPI

Article

Explainable AI-Enhanced Human Activity Recognition for Human–Robot Collaboration in Agriculture

Lefteris Benos [1,*], Dimitrios Tsaopoulos [1], Aristotelis C. Tagarakis [1], Dimitrios Kateris [1], Patrizia Busato [2] and Dionysis Bochtis [1,3]

[1] Institute for Bio-Economy and Agri-Technology (IBO), Centre of Research and Technology-Hellas (CERTH), 6th km Charilaou-Thermi Rd., 57001 Thessaloniki, Greece; d.tsaopoulos@certh.gr (D.T.); a.tagarakis@certh.gr (A.C.T.); d.kateris@certh.gr (D.K.); d.bochtis@certh.gr (D.B.)
[2] Interuniversity Department of Regional and Urban Studies and Planning (DIST), Polytechnic of Turin, Viale Mattioli 39, 10125 Torino, Italy; patrizia.busato@polito.it
[3] farmB Digital Agriculture S.A., 17th November 79, 55534 Thessaloniki, Greece
* Correspondence: e.benos@certh.gr

Abstract: This study addresses a critical gap in human activity recognition (HAR) research by enhancing both the explainability and efficiency of activity classification in collaborative human–robot systems, particularly in agricultural environments. While traditional HAR models often prioritize improving overall classification accuracy, they typically lack transparency in how sensor data contribute to decision-making. To fill this gap, this study integrates explainable artificial intelligence, specifically SHapley Additive exPlanations (SHAP), thus enhancing the interpretability of the model. Data were collected from 20 participants who wore five inertial measurement units (IMUs) at various body positions while performing material handling tasks involving an unmanned ground vehicle in a field collaborative harvesting scenario. The results highlight the central role of torso-mounted sensors, particularly in the lumbar region, cervix, and chest, in capturing core movements, while wrist sensors provided useful complementary information, especially for load-related activities. The XGBoost-based model, selected mainly for allowing an in-depth analysis of feature contributions by considerably reducing the complexity of calculations, demonstrated strong performance in HAR. The findings indicate that future research should focus on enlarging the dataset, investigating the use of additional sensors and sensor placements, and performing real-world trials to enhance the model's generalizability and adaptability for practical agricultural applications.

Keywords: XGBoost classification; SHapley Additive exPlanations (SHAP); feature importance; field experiment; material handling tasks; wearable sensors; multi-sensor information fusion; human factors

Academic Editor: Wojciech Kolanowski

Received: 9 December 2024
Revised: 7 January 2025
Accepted: 10 January 2025
Published: 10 January 2025

Citation: Benos, L.; Tsaopoulos, D.; Tagarakis, A.C.; Kateris, D.; Busato, P.; Bochtis, D. Explainable AI-Enhanced Human Activity Recognition for Human–Robot Collaboration in Agriculture. *Appl. Sci.* **2025**, *15*, 650. https://doi.org/10.3390/app15020650

1. Introduction

As a means of overcoming the challenges arising from the dynamic, unstructured, and unpredictable nature of open-field agricultural environments [1,2], humans and robots should work collaboratively [3–5]. Human–robot interaction (HRI) brings together the unique cognitive abilities of humans, such as perception and critical judgment, and the strengths of robots, including precision, consistency, and physical power [6,7]. This fusion creates a synergistic partnership that offers numerous benefits, such as greater flexibility for system reconfiguration, the optimized use of workspace, boosted productivity, faster return on investment, and the development of advanced, skill-intensive job opportunities [8–10].

A key aspect of effective and seamless HRI is human activity recognition (HAR), which involves identifying human body movements, activities, and gestures through data collected from various sensors, such as cameras and wearable devices [11,12]. By understanding human actions, robots can respond appropriately and align their actions with workers' activities, adapting dynamically without requiring explicit instructions [13,14]. This adaptability is vital in unpredictable agricultural environments, where human activities can also vary significantly. Furthermore, HAR significantly enhances both perceived safety (humans feel safe when working alongside robots) and trust (confidence in the reliability and predictability of the robots) in collaborative environments [15,16].

Recently, there has been a growing interest in HAR within the agricultural sector. With a focus on the related literature, to meet the demand for more intuitive communication systems that facilitate HRI, a vision-based approach for recognizing static hand gestures was introduced in [17]. To overcome limitations concerning capturing the full spectrum of human intentions during continuous tasks, dynamic movement recognition systems were introduced in [18,19], integrating a wider variety of body movements. This advancement enabled detailed and accurate interactions between humans and robots in harvesting operations. Despite the encouraging results, the above studies faced challenges due to the use of RGB-D cameras, which struggled with environmental variations like changing lighting and background conditions.

In response to these issues, wearable sensors have emerged as a promising alternative for HAR in agriculture. These sensors provide additional data layers that enhance HAR, even in suboptimal conditions such as those with low lighting or obstructions. However, challenges remain mainly in sensor data fusion, potential drift, synchronization, and the increased computational burden associated with processing multi-sensor data. For example, hand gesture recognition was accomplished using data from sensors embedded in a specialized glove to control a robotic arm for weed removal in [20]. In [21], a shirt with an attached smartphone was used to collect acceleration signals during various material handling tasks. Similarly, Sharma et al. [22–24] utilized accelerometer data, along with inputs from microphones and GPS on smartphones, to evaluate the performance of different ML algorithms. Accelerometers, placed on the wrists, were also used in [25] for classifying specific activities of agricultural operators using vibrating tools. Field experiments in [26,27] involved collecting data with wearable sensors (accelerometers, gyroscopes, and magnetometers) during a collaborative human–robot harvesting scenario. In these investigations, the obtained data were processed using a Long Short-Term Memory (LSTM) network to enable HAR through the integration of multiple data modalities, while additionally, optimal sensor placement was investigated in [27].

The common denominator of the above studies is that HAR relies on ML classifiers to analyze data from various sources. Specifically, ML models, primarily based on supervised learning techniques, are trained on labeled datasets to recognize patterns and accurately classify different activities. In multi-sensor HAR systems, individual sensors typically consist of multiple physical channels to process the various directional components of motion signals. As a result, processing multi-channel signals and extracting relevant features are essential prerequisites. Nevertheless, the importance of physical channels often varies significantly, as not all channels contribute equally to the activity. A challenge arises from the independent processing of each channel, as the most relevant channels may be distributed across different sensors, complicating the process of sensor selection [28,29]. Moreover, in practical applications, energy consumption cannot be minimized effectively, since all channels within a sensor remain active. Consequently, a key limitation of these models is their "black-box" nature, meaning that the decision-making process is often not transparent or interpretable [30,31]. This lack of explainability can be problematic,

especially in high-risk environments like agriculture, because it can hinder trust and safety, as well as learning and improvement.

To tackle the aforementioned limitations, the present study leverages explainable artificial intelligence (XAI) for the first time in the relevant literature, to the best of the authors' knowledge. Specifically, we employed the SHapley Additive exPlanation (SHAP) method in combination with an eXtreme Gradient Boosting (XGBoost) classifier to analyze a dataset collected for HAR. The analyzed activities pertain to a collaborative human–robot setting, where an unmanned ground vehicle (UGV) assisted workers during the harvesting process by transporting full crates, as described in [32–34]. The calculation of SHAP values provides insights into sensor and channel importance, enabling the optimization of sensor selection and feature relevance. Overall, this approach contributes to the development of more efficient and energy-conscious HAR systems tailored for real-world agricultural applications. Concerning data collection, the data were gathered during outdoor experimental sessions in which twenty participants took part, each outfitted with five inertial measurement units (IMUs) placed at various positions of the body, alongside a UGV. Finally, to encourage further research, the dataset used in this study has been made publicly accessible in [35].

The structure of the remainder of this paper is as follows: Section 2 outlines the methodology for data collection, data pre-processing, and the development of the XGBoost-based HAR model, alongside the SHAP framework used to interpret the model. Section 3 presents the key findings from the SHAP-enhanced XGBoost model. Section 4 discusses the results in a broader context and explores potential directions for future research, while Section 5 concludes with the main insights from the study.

2. Materials and Methods

The end-to-end workflow of the proposed XGBoost-based HAR framework, also incorporating SHAP for interpretability, is summarized in Figure 1, with a brief explanation of the key steps—(a) data acquisition; (b) data pre-processing and feature extraction; (c) XGBoost model training; (d) model evaluation; and (e) explainability—provided in the following subsections.

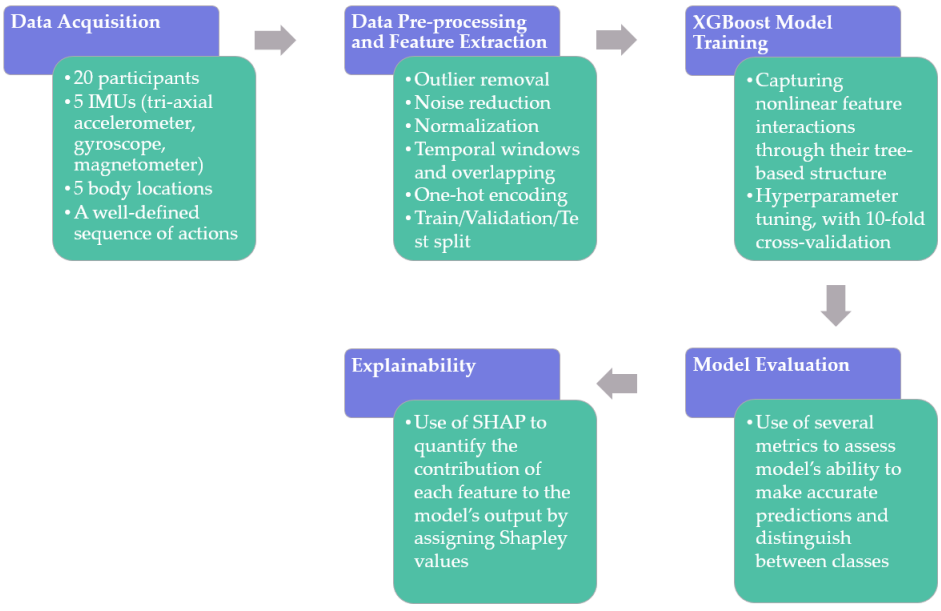

Figure 1. End-to-end workflow of the proposed explainable artificial intelligence-based human activity recognition framework.

2.1. Data Acquisition

The field experimental sessions, described in detail in [27], took place on a farm located in central Greece. In short, a total of 20 participants (10 males, 10 females) voluntarily took part in the experiments. The selection of participants with diverse characteristics, including variations in gender, age, weight, and height, was deliberate, ensuring that the data collected represented a broad spectrum of variability. The participants had an average age of 30.13 years (standard deviation (SD) ≈ 4.13 years), an average weight of 70.2 kg (SD ≈ 16.1 kg), and an average height of 1.71 m (SD ≈ 0.10 m). Eligibility for the study required all individuals to be free from any musculoskeletal injuries or surgical procedures within the past year that could impair their physical performance. Before the experiments began, all participants gave their informed consent, with the study protocol receiving prior approval from the Institutional Ethical Committee. Each participant was also required to engage in a five-minute warm-up before commencing the testing procedures to help prevent injuries [36,37].

The participants were instructed to perform the following sequence of actions: (1) stand still until the start signal; (2) walk 3.5 m in a straight line; (3) lean down to pick up a crate; (4) lift the crate to a standing posture; (5) carry the crate while walking back 3.5 m; and (6) position the crate on the available UGV. The individuals were required to carry either an empty crate weighing 1.5 kg or a crate loaded with weight plates, totaling one-fifth of their body mass [38,39]. Weight adjustments were made using 1 kg and 2.5 kg plates for precise calibration. Each participant completed both scenarios (one with an empty crate and one with a loaded crate) three times each in a random sequence, allowing them to set their own pace throughout the process. The experimental setup utilized a commonly used UGV (Thorvald, SAGA Robotics SA, Oslo, Norway), depicted in Figure 2, for agricultural field applications, which featured a crate deposit height of 80 cm.

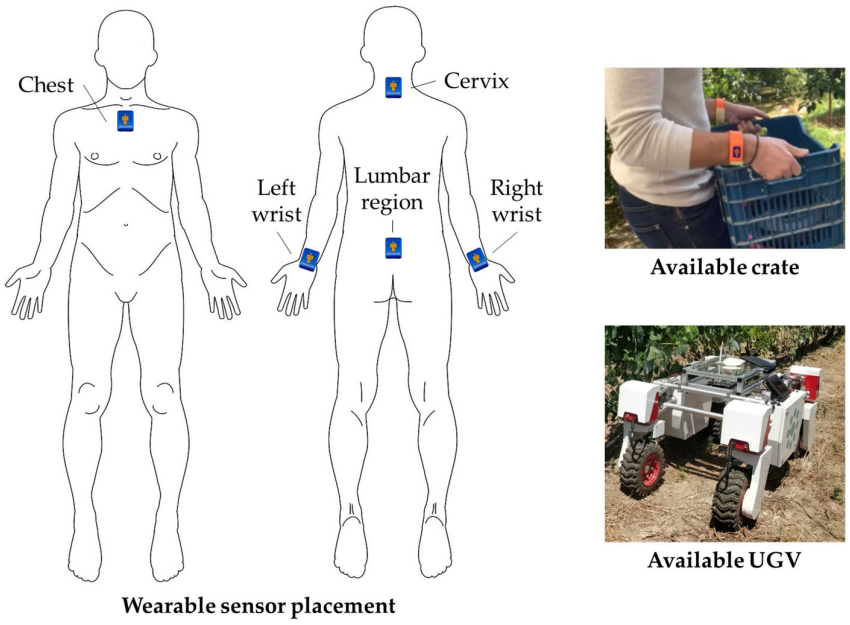

Figure 2. A visual representation of the wearable sensors' placement on the human body along with the available crate and unmanned ground vehicle (UGV) used in the experimental sessions.

For data collection, five IMUs (Blue Trident, Vicon, Nexus, Oxford, UK), normally used in similar studies [40–42], were employed. Each IMU contained a tri-axial accelerometer (measured magnitude: acceleration; range/units: ± 16 g; sensitivity: 16-bit), gyroscope (measured magnitude: angular velocity; range/units: ±2000 °/s; sensitivity: 16-bit), and magnetometer (measured magnitude: direction/position; range/units: ± 4900 μT; sensitiv-

ity: 16-bit), allowing for detailed motion tracking along three axes [43]. The 50 Hz sampling rate ensured adequate temporal resolution for capturing the dynamics of the movements performed within the scope of this study [26,39]. The data collected by the five IMUs (in CSV format) were stored directly on each sensor, with each file containing information about the specific body location. The sensors were interfaced with a data acquisition system connected to a computer for offline analysis. Capture.U software 1.4.1 [44] was used to synchronize the IMUs, while its installation on an Apple iPad mini (64 GB) facilitated the simultaneous recording of video during the experiments. This feature provided a clear visual cue, enabling the manual segmentation of the activity data into distinct epochs and the precise localization of temporal events marking transitions between activities.

The activities to be recognized were as follows:

1. Standing still (Class 0): the participant remains stationary without movement, awaiting the start signal to initiate the task;
2. Walking without a crate (Class 1): this activity begins when one foot makes contact with the ground to support the participant's body weight, while the other foot prepares to lift off for the subsequent step;
3. Bending to approach an empty crate (Class 2): this activity is marked by the participant initiating trunk flexion, knee flexion, or a combination of both;
4. Bending to approach a full crate (Class 3): this activity follows the same criteria as activity 3, but involves a full crate instead of an empty one;
5. Lifting an empty crate (Class 4): this activity involves transitioning from a bent posture to an upright standing position while lifting the crate;
6. Lifting a full crate (Class 5): The criteria for this activity are identical to those of activity 5, but with a full crate instead of an empty one;
7. Walking with an empty crate (Class 6): the stance phase of gait marks the onset of this activity, similarly to activity 2, but while carrying an empty crate;
8. Walking with a full crate (Class 7): this activity is similar to activity 7 but performed while carrying a full crate;
9. Placing an empty crate onto the UGV (Class 8): task initiation is marked by the onset of trunk or knee flexion by the participant to initiate the lowering of the crate, and the task terminates upon the successful deposition of the empty crate on the robotic system;
10. Placing a full crate onto the UGV (Class 9): this activity follows the same criteria as activity 9 but involves a full crate instead of an empty one.

As compared to the ML algorithm used in [26,27], the algorithm developed in this study not only recognizes distinct activities but also differentiates between handling an empty or full crate, thereby introducing four additional classes to the ML model. Recognizing heavier loads allows robots to provide timely assistance, reducing ergonomic stress on human workers [8]. Moreover, distinguishing crate types facilitates more efficient load management, enabling robots to optimize their movements and conserve energy. In dynamic agricultural workflows, identifying the weight of a crate could also help robots anticipate human intentions, improving coordination and promoting smoother interactions. Importantly, since empty and full crates correspond to different stages of the harvesting process, this differentiation aids in task prioritization and workflow optimization, ultimately making the system more robust and better suited to the practical demands of real-world agricultural environments [6].

To optimize data acquisition with a limited sensor array, the sensor placement strategy prioritized the upper-body and core regions to capture the activities under investigation. As detailed in [27], the sensor positioned over the sternum yields critical insights into whole-body movements and postural adjustments. The neck sensor, near the T1 vertebra, captures upper-body movements and alignment, which are important for actions such

as bending and lifting. The lumbar region sensor, positioned near the L4 vertebra, helps monitor lower-back motion, which is crucial for material handling activities. Finally, the wrist sensors track detailed hand and arm movements, which are essential for tasks that require the precise handling and coordination of the crate. Wrist sensors were fastened in place using Velcro straps, as shown in Figure 1, while double-sided tape was used for the remaining sensors.

2.2. Machine Learning Workflow

2.2.1. Data Pre-Processing and Feature Extraction

The critical steps for preparing raw sensor data to be clean and consistent and generating supplementary features for input into the ML model to better identify hidden patterns are described in detail in [27]. In summary, these steps include managing outliers and unsynchronized sensor data to ensure data consistency, as well as aligning sensor readings to a common time frame. Outlier identification and elimination were implemented during the initial data pre-processing phase using a z-score-based statistical technique, which identifies data points that deviate significantly from the mean [45]. A median filter with eleven taps was applied to effectively reduce noise in the data while maintaining important details within the dataset [46]. Each window was assigned a label corresponding to the activity occurring during that period. A 50% overlap was applied between consecutive windows to enhance data representation. One-hot encoding was used to represent categorical variables, as they provide a clear and unambiguous way to encode non-numeric data into a format that can be easily interpreted by ML algorithms. The StandardScaler [47] was applied to ensure that each feature had a mean of zero and a standard deviation of one. Subsequently, we split the dataset into training, validation, and test sets using an 80/10/10 ratio [32]. Finally, feature selection was not explicitly performed in this study, as SHAP values naturally assess and highlight the most influential features [48].

2.2.2. XGBoost Model Training and Evaluation

The predictive model used in this study was XGBoost, which is an optimized implementation of gradient boosting designed for speed and accuracy, making it particularly suitable for tasks involving large, complex, and noisy sensor data with many features, including data taken using accelerometers, gyroscopes, and magnetometers. XGBoost models are adept at capturing nonlinear feature interactions through their tree-based structure [49]. The primary reason, however, for selecting XGBoost in this analysis was that it additionally integrates seamlessly with SHAP, allowing for an in-depth analysis of feature contributions by considerably reducing the complexity of calculations [32,33], as will be elaborated next.

As mentioned above, three datasets were created:

- Training set: this was used for model training and hyperparameter tuning, with 10-fold cross-validation applied to this set to optimize the model's configuration;
- Validation set: this was used for evaluating and selecting the best XGBoost model after hyperparameter tuning and for preventing overfitting;
- Test set: This set was kept completely separate from the training and validation processes. It was used for a final, unbiased evaluation of the model's generalization performance through a diverse set of relevant metrics.

2.3. Model Explainability Using SHapley Additive ExPlanations (SHAP)

SHAP serves as a prominent technique for enhancing the interpretability of ML models by elucidating their predictive rationale across various applications, including healthcare [50,51], the energy sector [52,53], economics [54,55], and HAR [32,33], to mention but a few. Inspired by cooperative game theory, SHAP assigns each feature a contribution

value that helps explain its impact on the final prediction. Specifically, SHAP values quantify each feature's contribution to a specific prediction by comparing the output of the model with and without the feature in question. These values are calculated by considering all possible combinations of features and evaluating the average effect of a given feature on the prediction [56]. The result is a set of feature importance scores that can be visualized to identify the most influential factors driving the model's predictions.

Given a set of measurements $x_i = x_{i,1} + x_{i,2} + \ldots + x_{i,F}$, the goal is to accurately classify the corresponding activity y_i from a set of potential activities $Y = \{1, 2, \ldots, m\}$, with $m = 10$ in our case. Each individual sample contains various measurements gathered from multiple sensing units $S_1, S_2, \ldots, S_K$. SHAP values for the j^{th} feature (with $j \in F$, where F is the set of all features in the model) are calculated for x_i as

$$\varphi_j(x_i) = \sum_{S \subseteq F \setminus \{j\}} \frac{|S|!(F - |S| - 1)!}{F!} \left(v\left(x_{i,S \cup \{j\}}\right) - v(x_{i,S}) \right) \quad (1)$$

The summation in Equation (1) iterates over all possible subsets (S) of features excluding feature j. It also considers the factorial (!) of the number of features: (a) in subset S; (b) not in subset S and not including feature j; and (c) in set F. The term $v\left(x_{i,S \cup \{j\}}\right) - v(x_{i,S})$ calculates the difference in the model's prediction when feature j is included in the set of considered features compared to when it is excluded [57]. Considering a multi-class classification problem such as the present one, a set of outputs is utilized, namely, $v_1, v_2, \ldots v_m$, one for each class, while for each output, a separate SHAP score is calculated as $\varphi_{j,1}(x_i)$, $\varphi_{j,2}(x_i), \ldots \varphi_{j,m}(x_i)$. Regarding the SHAP score, it can be positive or negative, reflecting whether a feature increases or decreases the model's output. However, its influence is evaluated based on its absolute value. The total SHAP value of a feature is determined by taking the average of the absolute SHAP scores across a validation dataset $x_1, x_2, \ldots x_n$, and summing these values across all classes:

$$\varphi_j = \frac{1}{n} \sum_{i=1}^{n} \sum_{l=1}^{m} \left| \varphi_{j,l}(x_i) \right|. \quad (2)$$

Considering the present study's focus on a tree-based XGBoost model for HAR, SHAP was selected as the most appropriate explainability method. Its unique advantages make it preferable over alternative techniques, such as Local Interpretable Model-agnostic Explanations (LIMEs), the Python library "ELI5", Layer-wise Relevance Propagation (LRP), CounterFactual Explanations (CFEs), and Anchor [58–60]. In short, LIMEs can suffer from instability and limited global interpretability (similar to Anchor). ELI5 is effective for simpler models but struggles with complex ones, like the one used in this study. LRP works well for neural networks but is less effective for tree-based models, while CFEs lack the granularity needed for detailed feature importance. In contrast, SHAP ensures reliable global interpretability and provides clear feature importance. The primary challenge in applying SHAP values in practice is their high computational cost [58]. In model-agnostic settings, calculating SHAP values has a complexity of $O(2^F)$, meaning that the computation grows exponentially as the number of features increases. However, if the structure of the model is known, this complexity can be significantly reduced by leveraging this information. For example, in tree-based models, like the XGBoost model utilized in the present study, the TreeSHAP algorithm [61] enables SHAP values to be computed more efficiently with a complexity of $O(D^2)$, where D represents the maximum depth of the tree [32].

The development, training, and evaluation of the XGBoost and SHAP models were carried out using Python, with the Scikit-learn library [62] being the main framework used.

3. Results

3.1. Machine Learning Model Performance

The classification report in Table 1 provides a detailed performance evaluation of the proposed XGBoost-based HAR model for each activity class, along with relevant metrics, all of which report on the test dataset. On the whole, the model demonstrates high accuracy (93%), reflecting its overall effectiveness in classifying most activities, with slight room for improvement in distinguishing activities with overlapping characteristics, as will be discussed next.

Table 1. Classification report for the proposed model's performance.

Activity	Precision	Recall	F1-Score
Standing still	0.94	0.96	0.95
Walking without a crate	0.96	0.97	0.97
Bending to approach an empty crate	0.89	0.85	0.87
Bending to approach a full crate	0.90	0.83	0.86
Lifting an empty crate	0.93	0.91	0.92
Lifting a full crate	0.93	0.92	0.92
Walking with an empty crate	0.90	0.91	0.90
Walking with a full crate	0.91	0.92	0.91
Placing an empty crate onto the UGV	0.93	0.85	0.89
Placing a full crate onto the UGV	0.91	0.92	0.92
Accuracy			0.93
Macro average	0.92	0.90	0.91
Weighted average	0.93	0.93	0.93

By employing confusion matrices, the performance of the ML model can be effectively visualized and evaluated, providing a clear representation of classification accuracy by showing the counts of true positives, false positives, true negatives, and false negatives for each class. In the present study, the confusion matrix shown in Figure 3 is of a 10 × 10 size, where 10 is the number of classes (activities) to be predicted. As can be inferred by the diagonal dominance, the proposed ML model indicates substantial performance. However, there are some misclassifications, like that between Class 0 (standing still) and Class 1 (walking without a crate). Furthermore, as expected, misclassifications are observed mainly between similar activities involving either a full or empty crate (i.e., (a) bending to approach an empty/full crate; (b) lifting an empty/full crate; (c) walking with an empty/full crate; and (d) placing an empty/full crate onto the UGV).

3.2. Model Explainability

3.2.1. Global Feature Importance: Overview of Key Features Across All Classes

From this point forward, our focus is shifted to utilizing the SHAP framework to understand the contribution of each feature, namely, the recordings of accelerometers, a, gyroscopes, g, and magnetometers, m, in each direction (x, y, z) worn at each body location (chest, cervix, lumbar region, right wrist, left wrist) to the model's output by assigning Shapley values. The global feature importance plot is shown in Figure 4 for the top 20 most important features out of a total of 45 features—(3 types of sensors) × (3 directions) × (5 body locations)—used in the model. The horizontal bars in Figure 4 represent the average impact of each feature on the model's output magnitude, aggregated across all samples. Obviously, "my_lumbar region", "my_cervix", and "my_chest" features prove to be the most impactful features, indicating their strong influence on the classification of the investigated human activities. This also demonstrates the impact of magnetometer measurements, a fact that is confirmed by the presence of 12 features associated with magnetometers in the list of the top 20 ones.

The dominant impact of magnetometers was also highlighted in [27]. Thus, it seems that although new—but similar—activities were added, as compared to the activities taken into account in [27], magnetometers still play a crucial role in HAR. Additionally, Benos et al. [27] proved that sensors worn on the chest, lumbar region, and cervix provide the most stable and consistent data, as their central location contributes to accurately capturing core movements. This is ascertained by the first three most impactful features in the present analysis.

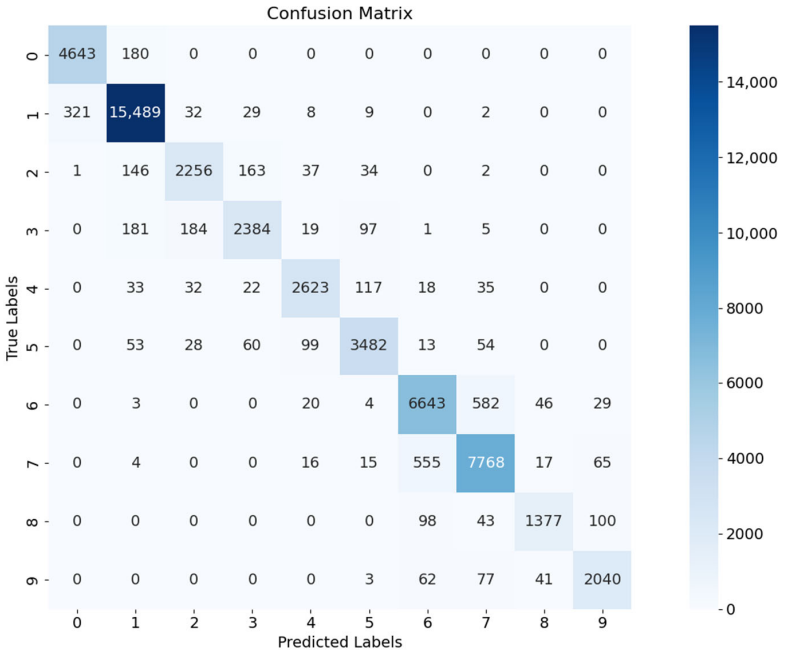

Figure 3. Confusion matrix for the employed XGBoost classifier with Class 0: standing still; Class 1: walking without a crate; Class 2: bending to approach an empty crate; Class 3: bending to approach a full crate; Class 4: lifting an empty crate; Class 5: lifting a full crate; Class 6: walking with an empty crate; Class 7: walking with a full crate; Class 8: placing an empty crate onto the UGV; Class 9: placing a full crate onto the UGV.

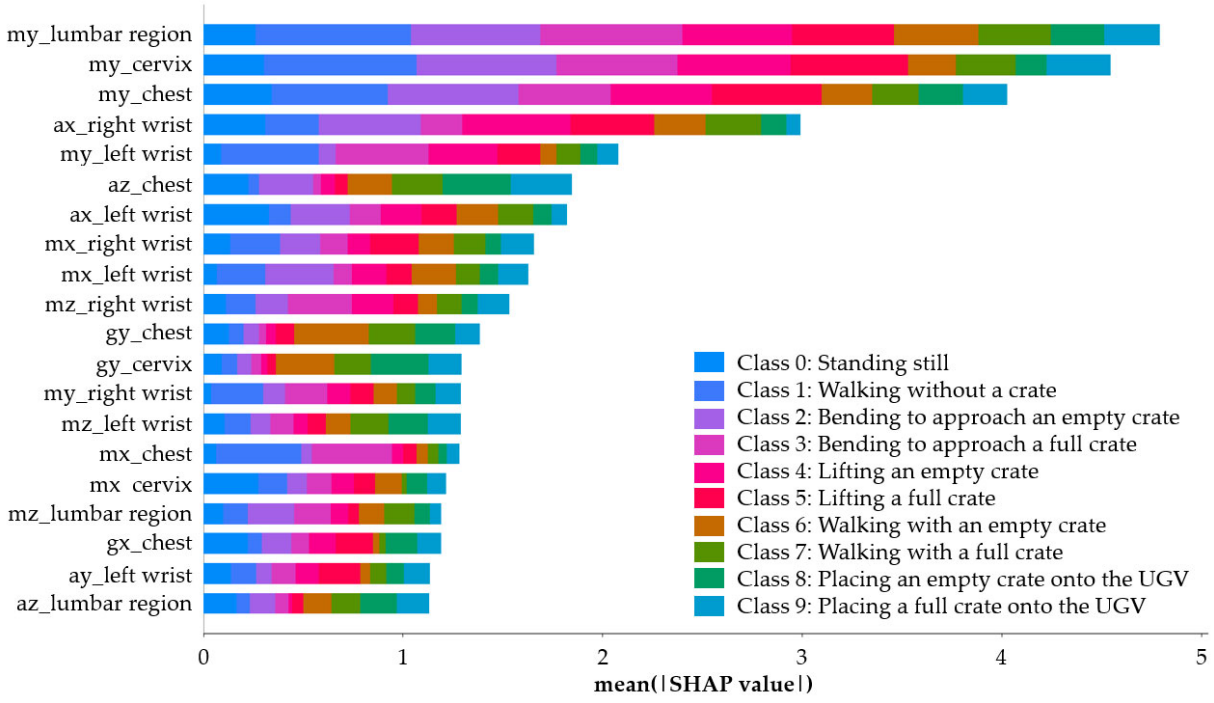

Figure 4. SHapley Additive exPlanation (SHAP) variable importance plot ranking the top 20 model features in decreasing order of contribution.

As noted in [27], sensors worn on the wrists presented challenges in recognizing clear patterns. In contrast, the present analysis, as shown in Figure 4, demonstrates that certain components of the IMUs worn on the wrists, particularly features like "ax_right_wrist" and "my_left_wrist", prove to be sufficiently important for classifying the examined activities. This difference can be attributed to the broader range of activities considered in the present study compared to [27]. While [27] focused on general activities, such as lifting a crate, bending to approach a crate, walking with a crate, and placing a crate onto a UGV, the current analysis introduces an additional layer of granularity by distinguishing between these activities based on the weight of the crate (full or empty). This level of detail allows the model to capture subtle variations in movement patterns linked to different task loads, making certain wrist-worn IMU components more relevant in classifying the activities.

On the other hand, the components with the least average impact on the model's output were "gy_left_wrist", "gy_right_wrist", and "gz_right_wrist". Interestingly, the gyroscopic sensors on both wrists do not make a significant contribution to the model's predictions, as they are not among the top features in terms of importance, as shown in Figure 4. Generally, features related to accelerometric, gyroscopic, and magnetometric data across various directions (x, y, z) exhibit varying levels of importance. This highlights the value of integrating data from multiple sensor modalities to achieve a more robust activity recognition model.

3.2.2. Evaluation of Class-Specific Feature Importance: Analyzing Feature Contributions for Each Activity Class

In this section, we delve into class-specific feature importance, focusing on the contributions of different sensor features for each individual class. Although this class-specific information is partially given in Figure 4, we examine each class separately for the sake of clarity. The SHAP variable importance plot ranking of the top five model features in decreasing order of contribution for Classes 0–9 is provided in Figure 5a–j. For "standing still" (Figure 5a), the most influential feature, namely, "my_chest", in conjunction with "my_cervix" and "mx_cervix", contributes significantly to the model's classification, likely due to the stable data provided by the chest sensor for this static activity. However, the wrist sensors, "ax_left_wrist" and "ax_right_wrist", are also important, displaying that while "standing still" is a low-movement activity, wrist sensors can still provide valuable information when paired with other body sensor data. For instance, they can help distinguish between "standing still" and other activities that involve similar body positions but different arm movements or body stances, which would be subtle in nature but impactful for classification. For the "walking without a crate" activity (Figure 5b), the top five features are "my_cervix", "my_chest", "my_lumbar region", "ax_right_wrist", and "mx_left_wrist". These features highlight the importance of sensors placed on the torso, mainly magnetometers, as they are crucial for capturing body movements during walking, while also, wrist sensors can capture arm swinging [63], a significant characteristic of walking.

Regarding both "bending to approach an empty/full crate" activities, the SHAP variable importance plots reveal significant contributions from similar features. In the empty-crate case (Figure 5c), the top features are "my_lumbar region", "gy_chest", "gy_cervix", "ax_right_wrist", and "my_chest", whereas in the full-crate case (Figure 5d), the top features are "my_lumbar region", "my_cervix", "ax_right_wrist", "az_chest", and "gy_chest". These results stress the importance of sensors placed on the torso, as the lumbar spine is highly involved in flexion and extension during such tasks, while the neck orientation helps in stabilizing body posture during the bending task [64,65]. In addition, the presence of the wrist sensor can be attributed to the different ways in which the hands are prepared to lift either an empty or full crate.

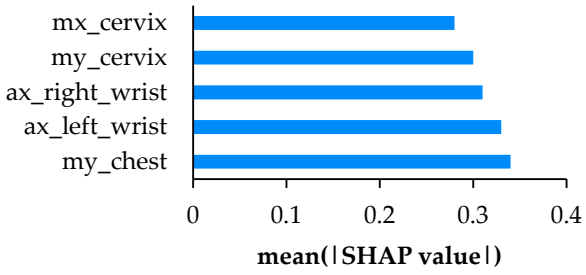

(**a**) Class 0: Standing still

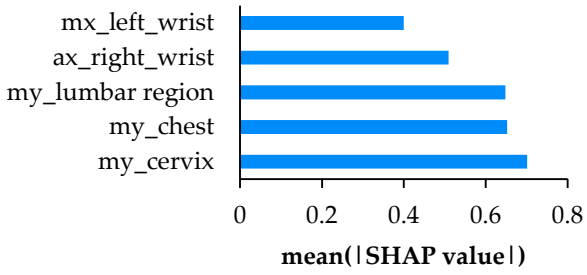

(**b**) Class 1: Walking without a crate

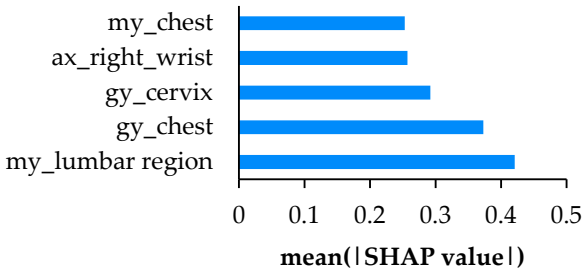

(**c**) Class 2: Bending to approach an empty crate

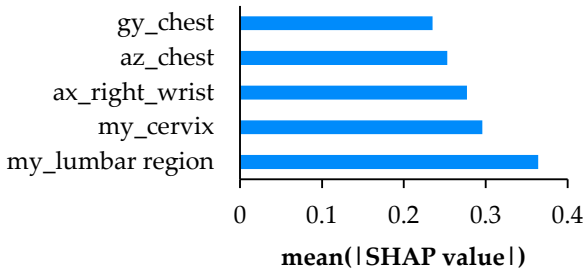

(**d**) Class 3: Bending to approach a full crate

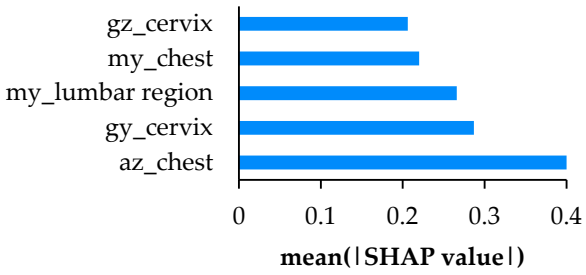

(**e**) Class 4: Lifting an empty crate

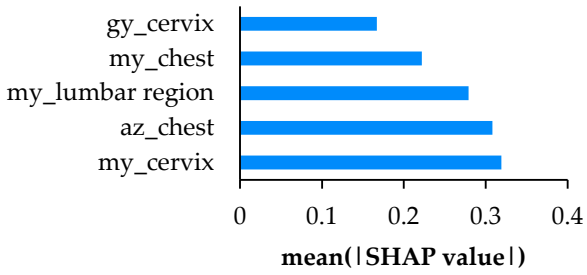

(**f**) Class 5: Lifting a full crate

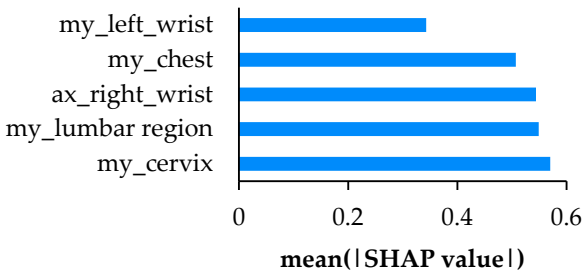

(**g**) Class 6: Walking with an empty crate

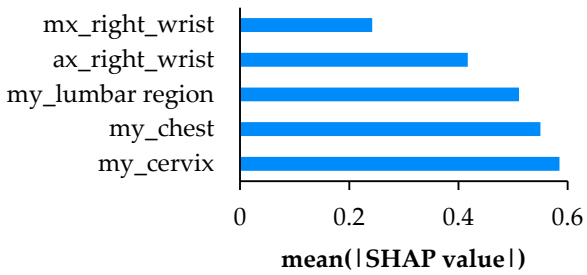

(**h**) Class 7: Walking with a full crate

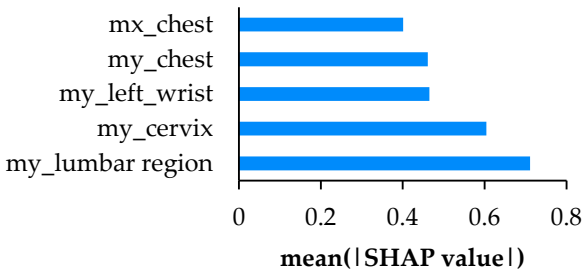

(**i**) Class 8: Placing an empty crate onto the UGV

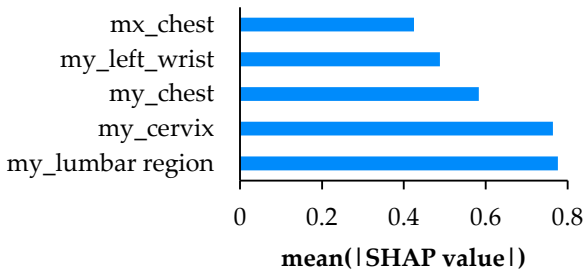

(**j**) Class 9: Placing a full crate onto the UGV

Figure 5. SHapley Additive exPlanation (SHAP) variable importance plot ranking the top 5 model features in decreasing order of contribution for each class.

The SHAP variable importance plots for both "lifting an empty/full crate" again disclose a consistent reliance on sensors placed on the torso, namely, on the lumbar region ("my_lumbar region"), chest ("my_chest" and "az_chest"), and cervix ("gy_cervix", "gz_cervix", and "my_cervix"). This result reflects the vertical, rotational, and stability-related movements required during lifting. Subtle differences arise in the handling of lighter (Figure 5e) versus heavier loads (Figure 5f), with adjustments in postural alignment and rotational coordination detected by the features.

Regarding both "walking with an empty/full crate", presented in Figure 5g,h, respectively, the role of torso sensors, particularly "my_cervix", "my_lumbar region", and "my_chest", is dominant in capturing key postural and movement dynamics during walking. These sensors likely reflect the body's adjustments to maintain balance and stability under varying loads. Wrist sensors, namely, "ax_right_wrist", "my_left_wrist", and "mx_right_wrist", also contribute, indicating the role of arm movements in stabilizing or carrying the crates. The subtle differences in feature contributions between the two activities suggest that heavier loads elicit distinct compensatory movements in both the torso and arms, reflecting the biomechanical adaptations required for load-bearing tasks [66,67].

Finally, for both "placing an empty/full crate onto the UGV", corresponding to Figure 5i,j, respectively, a consistent reliance on torso sensors is observed again, particularly "my_lumbar region" and "my_cervix, which are crucial for capturing core stability and postural adjustments during the task. The consistent contributions of "my_left_wrist" highlight the role of the wrists in facilitating the precise hand movements and coordination required to place the crate onto the UGV [27].

4. Discussion

4.1. Interpretation of the Results from a Broader Perspective

The present study provides a thorough evaluation of the proposed XGBoost-based HAR model, with a focus on understanding the underlying dynamics of feature contributions through XAI. In summary, the proposed model achieved a relatively high accuracy (93%) in classifying human activities, highlighting also its robustness in distinguishing between similar tasks. However, certain misclassifications were observed between similar activities involving subtle differences, such as bending or lifting an empty crate compared to a full crate. These misclassifications can be attributed to overlapping biomechanical patterns during these activities, emphasizing the complexity of accurately recognizing slight variations.

Beyond the commonly reported metrics for assessing the accuracy of the ML model, the approach adopted in this study offers significant value through its explainability, a feature notably absent in prior studies related to agriculture. The use of SHAP allowed for an in-depth understanding of the contributions of individual features. The global feature importance analysis highlighted the dominant role of magnetometer-based features, particularly those located in the lumbar region, cervix, and chest, which demonstrated their relevance in capturing core movements, as also pointed out in [26,27]. Magnetometers play a central role because they are effective in accurately determining orientation, rotational movements, and subtle changes in body posture [68,69]. These characteristics are essential for distinguishing between various human activities, especially those involving complex movements, such as bending, lifting, or carrying loads. Unlike accelerometers, which primarily measure linear acceleration, and gyroscopes, which detect angular velocity, magnetometers provide a reliable sense of directionality and spatial orientation. This makes them highly valuable for tasks requiring precise posture analysis and movement tracking, such as those performed in this study. However, the present study expanded on previous work [27] by identifying specific wrist sensor features, particularly all the

magnetometric components of both wrists as well as the "ax" component. This divergence is likely due to the broader range of activities considered in the present analysis, which includes differentiation based on crate weight.

4.2. Main Limitations of the Study

This study has some limitations that should be acknowledged. Firstly, it primarily relies on sensors placed on the chest, cervix, lumbar region, and both wrists, which may not capture the full spectrum of human movement, particularly in lower-body activities like walking. Sensor data quality and noise are other potential limitations, as variations in sensor placement can impact the accuracy of the model [70]. Furthermore, the model was evaluated on offline data, limiting its real-world applicability. Finally, the model's generalizability to diverse populations and conditions remains to be validated, as the training data may not reflect the full variability of human movement patterns.

4.3. Future Research Directions

The model's current performance could be further improved by incorporating a more diverse dataset that encompasses a wider range of agricultural material handling tasks in future research endeavors. For instance, the inclusion of older participants or individuals with different physical capabilities might reveal different movement patterns or physical limitations [71,72]. Investigating alternative sensor placements, mounted on lower extremities, could further optimize the combination of upper- and lower-body data, potentially identifying the most effective sensor configurations for different use cases. Exploring other sensor types, such as electromyography, could provide valuable complementary data, improving the model's accuracy for specific tasks [73,74]. Future research should also focus on addressing the challenges posed by possible sensor misplacement and variability in agricultural environments. Moreover, real-world experiments in agricultural collaborative robotics, combined with direct feedback from workers for also assessing the mental workload [75,76], are essential for addressing practical needs and usability challenges. For practical deployment, the Thorvald [77] or Husky robotic platforms [78] can be used for related agricultural tasks [26], as both are designed to support various sensors and autonomous operations in outdoor environments. Indicatively, multiple sensors such as LIDAR, RTK GPS, and IMUs for precise localization and navigation could be used. As presented in [18], the data collected by these sensors can be processed, for instance, by Jetson TX2 combined with CUDA, running a modified ROS Navigation Stack [79] with planners like TEB for obstacle avoidance [80]. Finally, integrating human intelligence and expertise into the robot's decision-making process through "human-in-the-loop optimization" can address the challenges of dynamic agricultural environments, foster user trust, and ensure safe, ethical robot behavior within adaptable, human-centered HRI systems [81–83].

5. Conclusions

The main objective of this study was to address the limitations of existing HAR models by incorporating XAI techniques. Specifically, its scientific novelty lies in the successful integration of SHAP into HAR within the context of human–robot collaboration in agriculture. By analyzing data and SHAP values collected from 20 participants wearing five IMUs on different body positions during outdoor agricultural tasks involving a UGV, this study offers valuable insights into the impact of sensor placement on activity recognition accuracy. The practical value of these findings is significant, as optimizing sensor placement improves the efficiency and cost-effectiveness of HAR systems, ultimately enhancing safety and performance in human–robot collaboration. In addition, the increased interpretability

of HAR models through SHAP analysis strengthens the reliability and robustness of the system, leading to more trustworthy activity recognition.

The main conclusions are outlined as follows:

- The XGBoost model exhibited a relatively high level of classification accuracy (93%) for all ten investigated activities;
- The use of SHAP allowed for deeper insights into feature contributions, emphasizing the significance of magnetometer-based features across various activities. Remarkably, the features "my_lumbar region", "my_cervix", and "my_chest" were identified as the most impactful;
- Sensors mounted on the torso, particularly on the lumbar region, cervix, and chest, proved to be critical for capturing core movements, while wrist sensors provided complementary information, especially for load-specific tasks;
- Future work should focus on expanding the dataset to include more activities and diverse participants to improve generalizability. Exploring additional sensors and experimenting with different sensor placements could enhance accuracy. Real-world testing in agricultural environments and long-term studies on system adaptability are also essential for practical applications.

Author Contributions: Conceptualization, L.B., D.T. and D.B; methodology, L.B. and D.T.; software, L.B.; validation, D.T. and A.C.T.; writing—original draft preparation, L.B.; writing—review and editing, L.B., D.T., A.C.T., D.K., P.B. and D.B.; visualization, L.B., D.K. and P.B.; supervision, D.B. All authors have read and agreed to the published version of the manuscript.

Funding: This research received no external funding.

Institutional Review Board Statement: This study was conducted according to the guidelines of the Declaration of Helsinki and approved by the Ethical Committee under the identification code 1660 on 3 June 2020.

Informed Consent Statement: Informed consent was obtained from all subjects involved in this study.

Data Availability Statement: The dataset used in this work is publicly available in [35].

Conflicts of Interest: Author Dionysis Bochtis is employed by the company farmB Digital Agriculture S.A. The remaining authors declare that the research was conducted in the absence of any commercial or financial relationships that could be construed as potential conflicts of interest.

References

1. Bechar, A.; Vigneault, C. Agricultural robots for field operations: Concepts and components. *Biosyst. Eng.* **2016**, *149*, 94–111. [CrossRef]
2. Bechar, A.; Vigneault, C. Agricultural robots for field operations. Part 2: Operations and systems. *Biosyst. Eng.* **2017**, *153*, 110–128. [CrossRef]
3. Aivazidou, E.; Tsolakis, N. Transitioning towards human–robot synergy in agriculture: A systems thinking perspective. *Syst. Res. Behav. Sci.* **2022**, *40*, 536–551. [CrossRef]
4. Seyyedhasani, H.; Peng, C.; Jang, W.; Vougioukas, S.G. Collaboration of human pickers and crop-transporting robots during harvesting—Part I: Model and simulator development. *Comput. Electron. Agric.* **2020**, *172*, 105324. [CrossRef]
5. Seyyedhasani, H.; Peng, C.; Jang, W.; Vougioukas, S.G. Collaboration of human pickers and crop-transporting robots during harvesting—Part II: Simulator evaluation and robot-scheduling case-study. *Comput. Electron. Agric.* **2020**, *172*, 105323. [CrossRef]
6. Benos, L.; Moysiadis, V.; Kateris, D.; Tagarakis, A.C.; Busato, P.; Pearson, S.; Bochtis, D. Human-Robot Interaction in Agriculture: A Systematic Review. *Sensors* **2023**, *23*, 6776. [CrossRef]
7. Yerebakan, M.O.; Hu, B. Human–Robot Collaboration in Modern Agriculture: A Review of the Current Research Landscape. *Adv. Intell. Syst.* **2024**, *6*, 2300823. [CrossRef]
8. Benos, L.; Bechar, A.; Bochtis, D. Safety and ergonomics in human-robot interactive agricultural operations. *Biosyst. Eng.* **2020**, *200*, 55–72. [CrossRef]

9. Salvine, P.; Nicolescu, M.; Ishiguro, H. Benefits of Human—Robot Interaction [TC Spotlight]. *IEEE Robot. Autom. Mag.* **2011**, *18*, 98–99. [CrossRef]
10. Marinoudi, V.; Benos, L.; Villa, C.C.; Lampridi, M.; Kateris, D.; Berruto, R.; Pearson, S.; Sørensen, C.G.; Bochtis, D. Adapting to the Agricultural Labor Market Shaped by Robotization. *Sustainability* **2024**, *16*, 7061. [CrossRef]
11. Singh, R.; Kumar Singh Kushwaha, A.; Chandni; Srivastava, R. Recent trends in human activity recognition—A comparative study. *Cogn. Syst. Res.* **2023**, *77*, 30–44. [CrossRef]
12. Huang, Y.; Zhou, Y.; Zhao, H.; Riedel, T.; Beigl, M. A Survey on Wearable Human Activity Recognition: Innovative Pipeline Development for Enhanced Research and Practice. In Proceedings of the 2024 International Joint Conference on Neural Networks (IJCNN), Yokohama, Japan, 30 June–5 July 2024; pp. 1–10.
13. Dahiya, A.; Aroyo, A.M.; Dautenhahn, K.; Smith, S.L. A survey of multi-agent Human–Robot Interaction systems. *Rob. Auton. Syst.* **2023**, *161*, 104335. [CrossRef]
14. Adamides, G.; Edan, Y. Human–robot collaboration systems in agricultural tasks: A review and roadmap. *Comput. Electron. Agric.* **2023**, *204*, 107541. [CrossRef]
15. Akalin, N.; Kristoffersson, A.; Loutfi, A. Do you feel safe with your robot? Factors influencing perceived safety in human-robot interaction based on subjective and objective measures. *Int. J. Hum. Comput. Stud.* **2022**, *158*, 102744. [CrossRef]
16. Benos, L.; Sørensen, C.G.; Bochtis, D. Field Deployment of Robotic Systems for Agriculture in Light of Key Safety, Labor, Ethics and Legislation Issues. *Curr. Robot. Rep.* **2022**, *3*, 49–56. [CrossRef]
17. Moysiadis, V.; Katikaridis, D.; Benos, L.; Busato, P.; Anagnostis, A.; Kateris, D.; Pearson, S.; Bochtis, D. An Integrated Real-Time Hand Gesture Recognition Framework for Human-Robot Interaction in Agriculture. *Appl. Sci.* **2022**, *12*, 8160. [CrossRef]
18. Moysiadis, V.; Benos, L.; Karras, G.; Kateris, D.; Peruzzi, A.; Berruto, R.; Papageorgiou, E.; Bochtis, D. Human–Robot Interaction through Dynamic Movement Recognition for Agricultural Environments. *AgriEngineering* **2024**, *6*, 2494–2512. [CrossRef]
19. Pal, A.; Leite, A.C.; From, P.J. A novel end-to-end vision-based architecture for agricultural human–robot collaboration in fruit picking operations. *Rob. Auton. Syst.* **2024**, *172*, 104567. [CrossRef]
20. Gokul, S.; Dhiksith, R.; Sundaresh, S.A.; Gopinath, M. Gesture Controlled Wireless Agricultural Weeding Robot. In Proceedings of the 2019 5th International Conference on Advanced Computing & Communication Systems (ICACCS), Coimbatore, India, 15–16 March 2019; pp. 926–929.
21. Patil, P.A.; Jagyasi, B.G.; Raval, J.; Warke, N.; Vaidya, P.P. Design and development of wearable sensor textile for precision agriculture. In Proceedings of the 2015 7th International Conference on Communication Systems and Networks, COMSNETS 2015–Proceedings, Bangalore, India, 6–10 January 2015; Institute of Electrical and Electronics Engineers Inc.: New York, NY, USA, 2015.
22. Sharma, S.; Raval, J.; Jagyasi, B. Mobile sensing for agriculture activities detection. In Proceedings of the 3rd IEEE Global Humanitarian Technology Conference, GHTC, San Jose, CA, USA, 20–23 October 2013; IEEE Computer Society: Washington, DC, USA, 2013; pp. 337–342.
23. Sharma, S.; Raval, J.; Jagyasi, B. Neural network based agriculture activity detection using mobile accelerometer sensors. In Proceedings of the 11th IEEE India Conference: Emerging Trends and Innovation in Technology, INDICON, Pune, India, 11–13 November 2014; Institute of Electrical and Electronics Engineers Inc.: New York, NY, USA, 2015.
24. Sharma, S.; Jagyasi, B.; Raval, J.; Patil, P. AgriAcT: Agricultural Activity Training using multimedia and wearable sensing. In Proceedings of the 2015 IEEE International Conference on Pervasive Computing and Communication Workshops, PerCom Workshops, St. Louis, MO, USA, 23–27 March 2015; Institute of Electrical and Electronics Engineers Inc.: New York, NY, USA, 2015; pp. 439–444.
25. Aiello, G.; Catania, P.; Vallone, M.; Venticinque, M. Worker safety in agriculture 4.0: A new approach for mapping operator's vibration risk through Machine Learning activity recognition. *Comput. Electron. Agric.* **2022**, *193*, 106637. [CrossRef]
26. Anagnostis, A.; Benos, L.; Tsaopoulos, D.; Tagarakis, A.; Tsolakis, N.; Bochtis, D. Human activity recognition through recurrent neural networks for human-robot interaction in agriculture. *Appl. Sci.* **2021**, *11*, 2188. [CrossRef]
27. Benos, L.; Tsaopoulos, D.; Tagarakis, A.C.; Kateris, D.; Bochtis, D. Optimal Sensor Placement and Multimodal Fusion for Human Activity Recognition in Agricultural Tasks. *Appl. Sci.* **2024**, *14*, 8520. [CrossRef]
28. Zhou, Y.; Yang, Z.; Zhang, X.; Wang, Y. A Hybrid Attention-Based Deep Neural Network for Simultaneous Multi-Sensor Pruning and Human Activity Recognition. *IEEE Internet Things J.* **2022**, *9*, 25363–25372. [CrossRef]
29. Zhou, Y.; Xie, J.; Zhang, X.; Wu, W.; Kwong, S. Energy-Efficient and Interpretable Multisensor Human Activity Recognition via Deep Fused Lasso Net. *IEEE Trans. Emerg. Top. Comput. Intell.* **2024**, *8*, 3576–3588. [CrossRef]
30. Marcus, E.; Teuwen, J. Artificial intelligence and explanation: How, why, and when to explain black boxes. *Eur. J. Radiol.* **2024**, *173*, 111393. [CrossRef]
31. Kök, İ.; Okay, F.Y.; Muyanlı, Ö.; Özdemir, S. Explainable Artificial Intelligence (XAI) for Internet of Things: A Survey. *IEEE Internet Things J.* **2023**, *10*, 14764–14779. [CrossRef]

32. Borella, E.; Çakmakçi, U.B.; Gottardis, E.; Buratto, A.; Marchioro, T.; Badia, L. Effective Sensor Selection for Human Activity Recognition via Shapley Value. In Proceedings of the 2024 IEEE International Workshop on Metrology for Living Environment (MetroLivEnv), Chania, Greece, 12–14 June 2024; pp. 22–27.
33. Arul, V.; Karthikeyan, P.; Ramanujam, E. Revealing the Importance of Local and Global Interpretability in Smartphone Based Human Activity Recognition. In Proceedings of the 2024 IEEE Students Conference on Engineering and Systems (SCES), Prayagraj, India, 21–23 June 2024; pp. 1–6.
34. Junaid, M.; Ali, S.; Eid, F.; El-Sappagh, S.; Abuhmed, T. Explainable machine learning models based on multimodal time-series data for the early detection of Parkinson's disease. *Comput. Methods Programs Biomed.* **2023**, *234*, 107495. [CrossRef]
35. Open Datasets—iBO. Explainable AI-Enhanced Human Activity Recognition for Human–Robot Collaboration in Agriculture. Available online: https://ibo.certh.gr/open-datasets/ (accessed on 7 January 2024).
36. Pedretti, A.; Gaya, A.C.A.; Mello, J.B.; Gaya, A.R. Effect of the PROFIT-BR exercise program on physical fitness of children: A protocol study. *BMC Sports Sci. Med. Rehabil.* **2024**, *16*, 203. [CrossRef]
37. Li, T.; Kapilevich, L.V.; Chen, J. Effects of Mild Fatigue on Biomechanics of Single Leg Landing in Young Male Volleyball Players. *Sensors* **2024**, *24*, 6811. [CrossRef]
38. Lavender, S.A.; Li, Y.C.; Andersson, G.B.; Natarajan, R.N. The effects of lifting speed on the peak external forward bending, lateral bending, and twisting spine moments. *Ergonomics* **1999**, *42*, 111–125. [CrossRef]
39. Tagarakis, A.C.; Benos, L.; Aivazidou, E.; Anagnostis, A.; Kateris, D.; Bochtis, D. Wearable Sensors for Identifying Activity Signatures in Human-Robot Collaborative Agricultural Environments. *Eng. Proc.* **2021**, *9*, 5. [CrossRef]
40. Slattery, P.; Cofré Lizama, L.E.; Wheat, J.; Gastin, P.; Dascombe, B.; Middleton, K. The Agreement between Wearable Sensors and Force Plates for the Analysis of Stride Time Variability. *Sensors* **2024**, *24*, 3378. [CrossRef] [PubMed]
41. Mascia, G.; De Lazzari, B.; Camomilla, V. Machine learning aided jump height estimate democratization through smartphone measures. *Front. Sports Act. Living* **2023**, *5*, 1112739. [CrossRef] [PubMed]
42. Salminen, M.; Perttunen, J.; Avela, J.; Vehkaoja, A. A novel method for accurate division of the gait cycle into seven phases using shank angular velocity. *Gait Posture* **2024**, *111*, 1–7. [CrossRef] [PubMed]
43. Blue Trident IMU | Inertial Sensor by Vicon | Biomechanic Tracking. Available online: https://www.vicon.com/hardware/blue-trident/ (accessed on 3 January 2024).
44. VICON Capture.U 1.4: IOS app for Blue Trident Sensors. Available online: https://www.vicon.com/software/captureu/ (accessed on 19 August 2024).
45. Sullivan, J.H.; Warkentin, M.; Wallace, L. So many ways for assessing outliers: What really works and does it matter? *J. Bus. Res.* **2021**, *132*, 530–543. [CrossRef]
46. El-Adawi, E.; Essa, E.; Handosa, M.; Elmougy, S. Wireless body area sensor networks based human activity recognition using deep learning. *Sci. Rep.* **2024**, *14*, 2702. [CrossRef]
47. Sklearn.preprocessing. StandardScaler—Scikit-Learn 0.24.1 Documentation. Available online: https://scikit-learn.org/stable/modules/generated/sklearn.preprocessing.StandardScaler.html (accessed on 20 January 2021).
48. Linardatos, P.; Papastefanopoulos, V.; Kotsiantis, S. Explainable AI: A Review of Machine Learning Interpretability Methods. *Entropy* **2021**, *23*, 18. [CrossRef]
49. Chen, T.; Guestrin, C. XGBoost: A Scalable Tree Boosting System. In Proceedings of the 22nd ACM SIGKDD International Conference on Knowledge Discovery and Data Mining, Barcelona, Spain, 25–29 August 2016; Association for Computing Machinery: New York, NY, USA, 2016; pp. 785–794.
50. Wu, X.; Ma, L.; Wei, P.; Shan, Y.; Chan, P.; Wang, K.; Zhao, G. Wearable sensor devices can automatically identify the ON-OFF status of patients with Parkinson's disease through an interpretable machine learning model. *Front. Neurol.* **2024**, *15*, 13887477. [CrossRef]
51. Liu, Z.; Zhang, Q.; Zheng, H.; Chen, S.; Gong, Y. A Comparative Study of Machine Learning Approaches for Diabetes Risk Prediction: Insights from SHAP and Feature Importance. In Proceedings of the 2024 5th International Conference on Machine Learning and Computer Application (ICMLCA), Hangzhou, China, 18–20 October 2024; pp. 35–38.
52. Cakiroglu, C.; Demir, S.; Hakan Ozdemir, M.; Latif Aylak, B.; Sariisik, G.; Abualigah, L. Data-driven interpretable ensemble learning methods for the prediction of wind turbine power incorporating SHAP analysis. *Expert Syst. Appl.* **2024**, *237*, 121464. [CrossRef]
53. Qiao, Q.; Eskandari, H.; Saadatmand, H.; Sahraei, M.A. An interpretable multi-stage forecasting framework for energy consumption and CO_2 emissions for the transportation sector. *Energy* **2024**, *286*, 129499. [CrossRef]
54. Li, X.; Deng, H.; Yu, X.; Yu, Y. Cooperative Impact of the Digital Sector, Eco-Friendly Policies, and Sophisticated Economic Development: A Study Drawing from China's Practices. *Sustainability* **2024**, *16*, 10525. [CrossRef]
55. Felix, J.; Alexandre, M.; Lima, G.T. Applying Machine Learning Algorithms to Predict the Size of the Informal Economy. *Comput. Econ.* **2024**, 1–21. [CrossRef]

56. Retzepis, N.-O.; Avloniti, A.; Kokkotis, C.; Protopapa, M.; Stampoulis, T.; Gkachtsou, A.; Pantazis, D.; Balampanos, D.; Smilios, I.; Chatzinikolaou, A. Identifying Key Factors for Predicting the Age at Peak Height Velocity in Preadolescent Team Sports Athletes Using Explainable Machine Learning. *Sports* **2024**, *12*, 287. [CrossRef] [PubMed]
57. Tatsuro, I. For a proof of unique existence. In *Game Theory for Economic Analysis*; Academic Press: New York, NY, USA, 1983; pp. 118–120, ISBN 0-12-370180-5.
58. Ali, S.; Abuhmed, T.; El-Sappagh, S.; Muhammad, K.; Alonso-Moral, J.M.; Confalonieri, R.; Guidotti, R.; Del Ser, J.; Díaz-Rodríguez, N.; Herrera, F. Explainable Artificial Intelligence (XAI): What we know and what is left to attain Trustworthy Artificial Intelligence. *Inf. Fusion* **2023**, *99*, 101805. [CrossRef]
59. Hassija, V.; Chamola, V.; Mahapatra, A.; Singal, A.; Goel, D.; Huang, K.; Scardapane, S.; Spinelli, I.; Mahmud, M.; Hussain, A. Interpreting Black-Box Models: A Review on Explainable Artificial Intelligence. *Cognit. Comput.* **2024**, *16*, 45–74. [CrossRef]
60. Mersha, M.; Lam, K.; Wood, J.; AlShami, A.K.; Kalita, J. Explainable artificial intelligence: A survey of needs, techniques, applications, and future direction. *Neurocomputing* **2024**, *599*, 128111. [CrossRef]
61. Lundberg, S.M.; Erion, G.; Chen, H.; DeGrave, A.; Prutkin, J.M.; Nair, B.; Katz, R.; Himmelfarb, J.; Bansal, N.; Lee, S.-I. From local explanations to global understanding with explainable AI for trees. *Nat. Mach. Intell.* **2020**, *2*, 56–67. [CrossRef]
62. Scikit-Learn, Machine Learning in Python. Available online: https://scikit-learn.org/stable/ (accessed on 1 November 2024).
63. Emmerzaal, J.; Filtjens, B.; Vets, N.; Vanrumste, B.; Smeets, A.; De Groef, A.; De Baets, L. A data-driven approach to detect upper limb functional use during daily life in breast cancer survivors using wrist-worn sensors. *Sci. Rep.* **2024**, *14*, 18165. [CrossRef]
64. Carnegie, D.R.; Hirsch, S.M.; Beach, T.A.; Howarth, S.J. Restricting lumbar spine flexion redistributes and changes total mechanical energy expenditure during lifting. *J. Biomech.* **2024**, *168*, 112132. [CrossRef]
65. Ojha, A.; Gautam, Y.; Jebelli, H.; Akanmu, A. Physiological impact of powered back-support exoskeletons in construction: Analyzing muscle fatigue, metabolic cost, ergonomic risks, and stability. *Autom. Constr.* **2024**, *168*, 105742. [CrossRef]
66. Benos, L.; Kokkotis, C.; Tsatalas, T.; Karampina, E.; Tsaopoulos, D.; Bochtis, D. Biomechanical Effects on Lower Extremities in Human-Robot Collaborative Agricultural Tasks. *Appl. Sci.* **2021**, *11*, 11742. [CrossRef]
67. Luo, Y.; Yang, F.; Yerebakan, M.O.; Zhang, J.; Hu, B. Load Carriage Modes and Limb Crossing Patterns Altered Gait during Obstacle Negotiation. *J. Mot. Behav.* **2022**, *54*, 525–536. [CrossRef] [PubMed]
68. He, Z.; Sun, Y.; Zhang, Z. Human Activity Recognition Based on Deep Learning Regardless of Sensor Orientation. *Appl. Sci.* **2024**, *14*, 3637. [CrossRef]
69. Khan, D.; Alshahrani, A.; Almjally, A.; Al Mudawi, N.; Algarni, A.; Alnowaiser, K.; Jalal, A. Advanced IoT-Based Human Activity Recognition and Localization Using Deep Polynomial Neural Network. *IEEE Access* **2024**, *12*, 94337–94353. [CrossRef]
70. Kumar, P.; Chauhan, S.; Awasthi, L.K. Human Activity Recognition (HAR) Using Deep Learning: Review, Methodologies, Progress and Future Research Directions. *Arch. Comput. Methods Eng.* **2024**, *31*, 179–219. [CrossRef]
71. Ofli, F.; Kurillo, G.; Obdržálek, Š.; Bajcsy, R.; Jimison, H.B.; Pavel, M. Design and Evaluation of an Interactive Exercise Coaching System for Older Adults: Lessons Learned. *IEEE J. Biomed. Health Inform.* **2016**, *20*, 201–212. [CrossRef]
72. Camp, N.; Lewis, M.; Hunter, K.; Johnston, J.; Zecca, M.; Di Nuovo, A.; Magistro, D. Technology Used to Recognize Activities of Daily Living in Community-Dwelling Older Adults. *Int. J. Environ. Res. Public Health* **2021**, *18*, 163. [CrossRef]
73. Rani, G.J.; Hashmi, M.F.; Gupta, A. Surface Electromyography and Artificial Intelligence for Human Activity Recognition—A Systematic Review on Methods, Emerging Trends Applications, Challenges, and Future Implementation. *IEEE Access* **2023**, *11*, 105140–105169. [CrossRef]
74. Xiong, D.; Zhang, D.; Chu, Y.; Zhao, Y.; Zhao, X. Intuitive Human-Robot-Environment Interaction with EMG Signals: A Review. *IEEE/CAA J. Autom. Sin.* **2024**, *11*, 1075–1091. [CrossRef]
75. Yerebakan, M.O.; Gu, Y.; Gross, J.; Hu, B. Evaluation of Biomechanical and Mental Workload During Human–Robot Collaborative Pollination Task. *Hum. Factors* **2024**, *67*, 100–114. [CrossRef]
76. Carissoli, C.; Negri, L.; Bassi, M.; Storm, F.A.; Delle Fave, A. Mental Workload and Human-Robot Interaction in Collaborative Tasks: A Scoping Review. *Int. J. Hum.–Comput. Interact.* **2024**, *40*, 6458–6477. [CrossRef]
77. Grimstad, L.; From, P.J. The Thorvald II Agricultural Robotic System. *Robotics* **2017**, *6*, 24. [CrossRef]
78. Reina, G.; Milella, A.; Galati, R. Terrain assessment for precision agriculture using vehicle dynamic modelling. *Biosyst. Eng.* **2017**, *162*, 124–139. [CrossRef]
79. Liu, Z.; Lü, Z.; Zheng, W.; Zhang, W.; Cheng, X. Design of obstacle avoidance controller for agricultural tractor based on ROS. *Int. J. Agric. Biol. Eng.* **2019**, *12*, 58–65. [CrossRef]
80. Xi, H.; Li, W.; Zhao, F.; Chen, L.; Hu, Y. A Safe and Efficient Timed-Elastic-Band Planner for Unstructured Environments. In Proceedings of the 2024 IEEE/RSJ International Conference on Intelligent Robots and Systems (IROS), Abu Dhabi, United Arab Emirates, 14–18 October 2024; pp. 3092–3099.
81. Slade, P.; Atkeson, C.; Donelan, J.M.; Houdijk, H.; Ingraham, K.A.; Kim, M.; Kong, K.; Poggensee, K.L.; Riener, R.; Steinert, M.; et al. On human-in-the-loop optimization of human–robot interaction. *Nature* **2024**, *633*, 779–788. [CrossRef]

82. Díaz, M.A.; Voß, M.; Dillen, A.; Tassignon, B.; Flynn, L.; Geeroms, J.; Meeusen, R.; Verstraten, T.; Babič, J.; Beckerle, P.; et al. Human-in-the-Loop Optimization of Wearable Robotic Devices to Improve Human–Robot Interaction: A Systematic Review. *IEEE Trans. Cybern.* **2023**, *53*, 7483–7496. [CrossRef]
83. Liebers, C.; Megarajan, P.; Auda, J.; Stratmann, T.C.; Pfingsthorn, M.; Gruenefeld, U.; Schneegass, S. Keep the Human in the Loop: Arguments for Human Assistance in the Synthesis of Simulation Data for Robot Training. *Multimodal Technol. Interact.* **2024**, *8*, 18. [CrossRef]